Molecular BioSystems

Accepted Manuscript

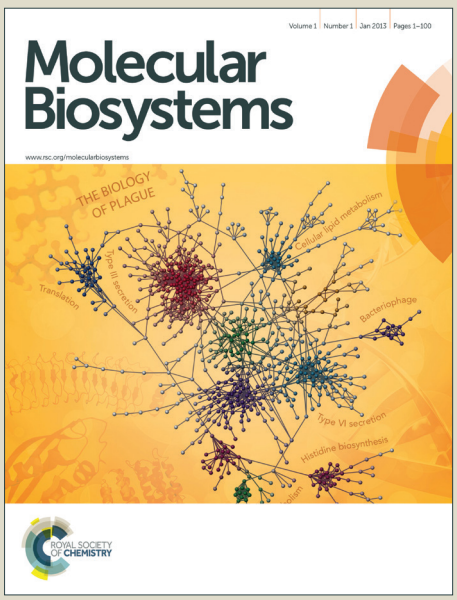

ROYAL SOCIETY OF CHEMISTRY

www.rsc.org/molecularbiosystems

Graphical abstract

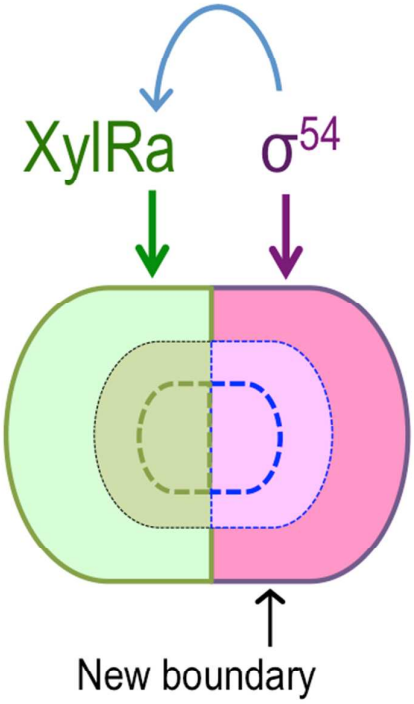

The functional boundaries of the *Pu* promoter can be expanded by overproduction of both sigma-54 and the transcriptional regulator XylR

Widening functional boundaries of the σ^{54} promoter *Pu* of *Pseudomonas putida* by defeating extant physiological constraints

by

Aitor de las Heras[1,2&], Esteban Martínez-García[1&], Maria Rosa Domingo-Sananes[3] and Víctor de Lorenzo[1*]

[1]*Systems Biology Program, Centro Nacional de Biotecnología-CSIC, Campus de Cantoblanco, Madrid 28049, Spain.* [2]*Synthetic and Systems Biology Centre and* [3]*Centre for Immunity, Infection and Evolution University of Edinburgh, EH93JT, UK*

Keywords: XylR, *Pseudomonas putida,* synthetic biology, regulatory feedback loops, biosensor, dynamic range

Running Title: Refactoring the *Pu* promoter of *P. putida*

* Correspondence to: Víctor de Lorenzo
Centro Nacional de Biotecnología-CSIC
Campus de Cantoblanco, Madrid 28049, Spain
Tel.: 34- 91 585 45 36; Fax: 34- 91 585 45 06
E-mail: vdlorenzo@cnb.csic.es

& These two Authors contributed equally to the work

ABSTRACT

The extant layout of the σ^{54} promoter *Pu*, harbored by the catabolic TOL plasmid pWW0, of *Pseudomonas putida* is one of the most complex instances of endogenous and exogenous signal integration known in the prokaryotic domain. In this regulatory system, all signal inputs are eventually translated into occupation of the promoter sequence by either of two necessary components: the *m*-xylene responsive transcriptional factor XylR and the σ^{54} containing form of RNA polymerase. Modelling of these components indicated that the *Pu* promoter could be upgraded to respond with much greater capacity to aromatic inducers by artificially increasing the endogenous levels of both XylR and the σ^{54} sigma factor, either separately or together. To explore these scenarios, expression of *rpoN*, the gene encoding σ^{54}, was placed under the control of an orthogonal regulatory system that was inducible by salicylic acid. We generated a knock-in *P. putida* strain containing this contstruct alongside the *xylR/Pu* regulatory module in its native configuration, and furthermore, a second strain where *xylR* expression was under the control of an engineered positive-feedback loop. These interventions allowed us to dramatically increase the transcriptional capacity (i.e. absolute promoter output) of *Pu* far beyond its natural scope. In addition, they resulted in a new regulatory device displaying more sensitive and ultra-fast responses to *m*-xylene. To our knowledge, this is the first time that the working regime of a promoter has been rationally modified by releasing the constraints imposed by its innate constituents.

INTRODUCTION

The functional space of every prokaryotic promoter is defined by a number of parameters that frame its performance *in vivo.* Promoters are rarely constitutively active[1] and are typically integral components of regulatory devices that respond to- and integrate external physiological and environmental signals to dictate transcription initiation[2-4]. Such signals can be both endogenous and exogenous and either physicochemical or nutritional[3]. In order to sense such cues and provide suitable responses, promoters perform distinct signal-processing tasks that are implemented through the interaction of a suite of transcription factors (TFs) with the RNA polymerase and target DNA sequences[1, 4-6]. Yet, the actual activity boundaries of each promoter are defined by the biological function that the respective regulatory node has evolved to deliver. This is implemented through the interplay between signal-specific and global control machinery inside the specific regulatory system[7, 8], the connectivity of which determine the fine-tuning of the transcriptional outcome[9, 10]. However, the functional parameters exhibited by extant individual promoters that have evolved to reach an optimal performance in its host bacterium does not preclude the ability of the promoter to physiologically operate beyond such natural constraints.

To explore whether working boundaries of regulatory nodes can be expanded by removal of extant physiological constraints we have focused on the *Pu* promoter of the soil bacterium *Pseudomonas putida*. This promoter is one of the most sophisticated examples of processing internal and external cues in a single regulatory element and is contained within the TOL plasmid pWW0[11]. For this bacterium, *Pu* and the various factors it interacts with (Fig. 1), form the primary sensor/actuator device of a complex metabolic and regulatory network that determines a pathway for biodegradation of *m*-xylene[11]. The route encompasses two catabolic operons, which are subject to a complex regulatory circuit that involves the interplay between plasmid-encoded and chromosome-encoded regulatory proteins[11-14]. The key event that triggers activation of the pathway is the interaction of the substrate (*m*-xylene) with the master TF of the system, called XylR. This TF is a member of the prokaryotic enhancer-binding protein family of regulators[15-17] that act in concert with the RNA polymerase (RNAP) containing the alternative σ^{54} sigma factor[13, 17]. Both σ^{54}-RNAP and XylR then sit at distant places of the DNA sequence *Pu* promoter to form a tridimensional transcription initiation complex with the assistance of the DNA-bending factor IHF (integration host factor[18, 19]). Purified σ^{54}-RNAP, IHF and activated XylR have the ability to activate the *Pu* promoter *in vitro* [20]. *In vivo,* however, the binding of XylR to its respective sites in the promoter is

regulated by the action of a number of factors (Fig. 1). These hinder XylR attachment to DNA in a manner dependent upon numerous physiological conditions[12, 21, 22]. Nevertheless, intracellular XylR levels are subject themselves to fine transcriptional and post-transcriptional regulation (Fig. 1) that indirectly controls the number of molecules of the TF that are available for sensing *m*-xylene and binding *Pu*. One of the key features of *xylR* expression is that *m*-xylene activated XylR represses its own transcription from its P_R promoter[23-25]. In contrast, *in vivo* binding of RNAP-σ^{54} to *Pu* is additionally regulated through various factors. Beyond providing architectural assistance to interact with distantly-bound XylR, IHF also helps σ^{54}-RNAP to bind its target -12/-24 sequence in *Pu*[26-28]. As a consequence, a better DNA binding site overcomes the need for IHF[29]. Finally, the share of σ^{54}-RNAP in the pool of available polymerase is controlled by sigma factor competition; a process controlled itself by ppGpp and the RNAP-associated factor DksA[30-32]. All these *in vivo* elements that operate on *Pu* confine its activity profile to a limited number of native functional states[33] that deliver the restricted transcriptional capacity, effector sensitivity/specificity and time of response that we observe in *P. putida*.

Given that optimal promoter performance can be obtained through occupation of *Pu* by *m*-xylene-activated XylR and σ^{54}-RNAP, we wondered whether artificially favouring such occupancy *in vivo* could reveal the maximum functional promoter capability when removed of native regulatory constraints. Indeed, enhancing the levels of both XylR and RNAP-σ^{54} can theoretically out-compete their binding antagonists to *Pu* by mere kinetic displacement of the corresponding DNA sites (Fig. 1). In this work we have investigated whether we could upgrade the transcriptional performance of *Pu in vivo* beyond native regulatory constraints by manipulating the intracellular concentrations of XylR and σ^{54}. To this end, we first explored with a simple mathematical model whether the innate output of the XylR/*Pu* device could be modified by increasing alternatively σ^{54}, XylR or both. We further explored this promoter system using a suite of genetic constructs engineered within transposon vectors encoding *xylR* and *rpoN* (the σ^{54} gene) under the control of different expression circuits. As shown below, this approach allowed us not only to increase the net output of the XylR/*Pu* regulatory node in *P. putida* but also, endow the system with an ultra-fast and super-sensitive response to the aromatic inducer. We thus argue that the native regulatory constraints governing the functional capability of given promoters *in vivo* can be manipulated through improving the DNA sequences bound by TFs, but also by rationally changing their genetic wiring.

RESULTS AND DISCUSSION

Signal-specific and overall functional boundaries of the XylR/Pu regulatory node

The principal actors of the regulation of the *XylR/Pu* device, which controls expression of the TOL pathway genes contained in the pWW0 plasmid of *P. putida*, are shown in Fig. 1. The default minimum promoter only requires XylR and σ^{54}-RNAP binding to DNA. This primes *Pu* to respond to *m*-xylene, however a large number of overall physiological signals also influence the system by [i] controlling intracellular XylR levels, [ii] impeding binding of XylR to its target sequences to *Pu*, [iii] easing the docking of σ^{54}-RNAP through interactions of the N-domain of its α subunit with a UP element and [iv] restricting the share of σ^{54}-containing species in the whole RNAP pool available for *Pu* binding. Signal integration is thus eventually translated into the variable association of the two key players of transcriptional initiation: σ^{54}-RNAP and XylR. This is made possible by their low abundance *in vivo*: 80 σ^{54} molecules[34] and 30-140 XylR monomers[35] per cell. This native scenario limits the system within given functional parameters. But at the same time, changes in the levels of either of σ^{54}-RNAP or XylR can make a considerable difference in the observed behaviour of the system. This raises the question of whether one can alter promoter performance by manipulating the cues that are channeled through available σ^{54}-RNAP, which itself depends on σ^{54} binding to the core enzyme, or through XylR. In the work below we consider the two scenarios, first by separate and then together.

Increasing σ^{54} levels enhances transcriptional output of the XylR/*Pu* node

An earlier indication of the effect of artificially high levels of σ^{54} on *Pu* was hinted at by Cases *et al*[36], who showed that rising the *in vivo* concentration of the factor by means of an IPTG-inducible expression system relieved the exponential silencing of the promoter that is typically observed during fast growth in rich medium (*exponential silencing* was the term used at the time to signify the whole of physiological control[12]). In order to rigorously formalize the regulatory scenario under study, we first simulated the performance of promoters *Pu* and P_R following induction of the system with *m*-xylene (Fig. 2A). *Pu* activity is represented as emission of luminescence of a *Pu-luxCDABE* fusion, while the output of P_R was equal to production of XylR protein. Under the naturally occurring regulatory setting of Fig. 2A (i.e. the levels of σ^{54} are kept low and constant), addition of the aromatic inducer has two opposite

consequences: *Pu* activity increases, but XylR levels decrease because of the negative feedback loop of the TF in its own transcription. In a second simulation (Fig. 2B), we examined the effect of increasing artificially intracellular σ^{54} concentration (for instance, through an expression system dependent on an external inducer). The model predicts in this case that *Pu* output again rises, but the dynamics of XylR production remains impervious to the same perturbance i.e., there is no variation in P_R output and thus XylR levels behave as before.

In order to proofs these predictions and test the model with experimentally measured parameters we engineered a mini-Tn*5* transposon determining transcription of the *rpoN* gene (encoding σ^{54}) under the control of an expression system responding to salicylate[37] (Table 1). Both salicylate and the respective responding TF (the regulator called NahR) are entirely orthogonal to *P. putida* KT2440, thereby ensuring the specificity of the response once cells are exposed to the inducer. The transposon Tn*5* [Psal•RpoN] (module #4 in Fig. 3D) was then delivered to the chromosome of *P. putida* X•wt, a *Pu-luxCDABE* reporter strain in which the *xylR* gene is expressed under its naturally occurring P_R promoter (Table 1 and Fig. 3E) and resulted in strain *P. putida* Psal•RpoN•X•wt. To verify that knocking-in the Tn*5* [Psal•RpoN] module raised intracellular σ^{54} concentrations in this strain, we grew cells in the presence of salicylate using as a control the isogenic strain *P. putida* X•wt devoid of the heterologous expression system. The concentration of salicylate used (2 mM) was optimal for full induction of the *Psal* promoter[38]. Samples were then exposed or not to saturating vapours of *m*-xylene for establishing whether this TOL pathway substrate could have any influence on σ^{54} concentrations as well. After an induction period of 6 h, protein extracts of each culture were examined for levels of the sigma factor in a Western blot assay with a recombinant anti-σ^{54} antibody[34]. The results of Fig. 4A show that the salicylate-induced cells bearing the *Psal-rpoN* module increased σ^{54} contents by >4-fold with respect to those of the isogenic strain without the transposon. In contrast, the levels of the factor were not significantly altered by *m*-xylene, whether σ^{54} was made at wild-type levels or overproduced owing to Tn*5* [Psal•RpoN]. The same samples were tested in parallel for *Pu* activity using light emission as a proxy of transcription initiation (Fig. 4B). The data revealed that *Pu* output in the strain where σ^{54} had been augmented (*P. putida* Psal•RpoN•X•wt) was > 5-fold higher than the counterpart with the naturally occurring levels of the factor (*P. putida* X•wt). To further examine this *Pu* hyper-activation we recorded light emission of the two strains along time but using 3-methylbenzyl alcohol (3MBA) instead of *m*-xylene as the aromatic inducer of the regulatory device. Since 3MBA is a weaker effector of XylR[39], its use allowed us to zoom in the

earliest effects of its addition to both strains as shown in Fig. 5. Note that for a more stringent comparison of the two conditions, fold-induction (rather than specific luminescence) was plotted *vs.* time. The results demonstrate notable magnification of *Pu* activity by only increasing the σ^{54} pool. While *P. putida* X•wt displayed a higher induced activity (10 to 15-fold), the equivalent strain with a higher σ^{54} pool reached ~120-fold at its peak of activity (approx. 18 hours after induction). Note, however that light emission did not start taking off until 6 h after inducer addition. This indicated that the mere overproduction of the factor (and plausibly an improved availability of σ^{54}-RNAP for binding *Pu*) did not suffice to surmount all other physiological inputs that checked promoter activity *in vivo*. Still, the results of Fig. 5 show that a moderate overproduction of σ^{54} allowed a sustained uplifting of *Pu* output, i.e. that the functional limit imposed by its naturally low concentrations can be overcome and the activity space of the promoter thus expanded.

Merging augmented σ^{54} with genetically rewired XylR production

We next examined the second key actor of *Pu* activation: XylR. The general consensus rule of thumb regarding control of TF expression is that, unlike the promoters they control, the levels of regulators fluctuate between constrained limits. These generally do not exceed 2 to 4-fold variation, so that the activity landscape of every promoter is constrained by the immediate needs of the extant cellular economy[40, 41]. In the case of XylR, we have reported that transcription of the *xylR* varies, depending on growth phase within a 2 to 4-fold window[14], with a calculated number of molecules per cell fluctuating within the same range (30-140[35]). Such low levels not only cause considerable stochastic effects[42], but also make XylR binding to *Pu* to be weak[43] and easily competed out by other regulatory factors (Fig. 1). Artificially changing XylR levels is thus bound to have consequences. For instance, removal of the negative feedback loop that naturally rules *xylR* expression (Fig. 1) and its replacement by a self-induced positive feedback loop (PFL) that increases XylR upon exposure to cognate effectors increases the sensitivity and specificity of the regulatory node in response to aromatic inducers[39]. On this background we wondered about the effects of modifying simultaneously XylR levels (with PFL) and σ^{54} levels (with the *Psal-rpoN* construct).

As previous, we first simulated *Pu* output and XylR production under two artificial scenarios (the default wild-type scenario is simulated in Fig. 2A). In one case (Fig. 6A), *xylR* was under the control of *Pu*[39] and

therefore the innate limits imposed by self-regulation has been exchanged by a PFL (while σ^{54} levels are those of the wild type state). The instant consequence of this conversion is that XylR levels are predicted to grow when cells face *m*-xylene, a phenomenon that has been proven experimentally[39]. But at the same time, the scenario of Fig. 6A predicts an enhancement of *Pu* output comparable to that anticipated by increasing σ^{54} levels-only (Fig. 2B, note the different scales of Y axes). The situation changes considerably when an externally controlled increase of σ^{54} is knocked-in into the simulation (Fig. 6B). The model then predicts *Pu* output to be super-amplified because of two convergent effects. One is the sheer augmentation of the sigma factor that enlarges the share of σ^{54}-containing RNA for *Pu* binding as discussed above. But this same effect further increases XylR levels, as its expression is placed under the control of *Pu* in the engineered PFL. This makes *Pu* to reach a new maximum state that boosts its overall transcriptional output in respect to the wild-type situation. Simulations of Fig. 6 thus suggested that a high-capacity regime can be engineered by combining overproduction of σ^{54} with a *Pu*-driven expression of *xylR*. To test this experimentally we resorted to strains *P. putida* Pu•RBX (*Pu-luxCDABE* reporter bacteria in which the *xylR* gene is expressed through a *Pu*-driven PFL; Table 1 and Fig. 3E) and *P. putida* Psal•RpoN•Pu•RBX (same than Pu•RBX but inserted with Tn*5* [Psal•RpoN]; module #4 in Fig. 3D). As before, we grew these strains in the presence of 2 mM salicylic acid, added the cultures with the XylR effector 1 mM 3MBA and followed luminescence production along the next 16 h. The results, plotted as fold-induction *vs.* time, are shown in Fig. 7. Two salient features become evident. In one hand, inspection of strain *P. putida* Pu•RBX reveals that inducer-triggered XylR overproduction through the PFL engineered in the genetic module #3 [*Pu-xylR*] results in an increase of *Pu* inducibility in the same range (if slightly lower) than that observed in strain *P. putida* Psal•RpoN•X•wt as the consequence of increasing σ^{54}-only (cf. Fig. 5). But the second and more remarkable feature is that *P. putida* Psal•RpoN•Pu•RBX, which combines σ^{54} overproduction with the PFL that amplifies XylR levels, displays a still greater *Pu* output. While this behaviour was anticipated by the simulations of Fig. 6, the results of Fig. 7 exposed also an earlier response of the XylR/Pu device to inducer addition and a faster induction rate which were not predicted in the simplified model. Still, this effect is easy to explain mechanistically, as augmented levels of XylR and σ^{54}-RNAP are likely to displace other factors bound to *Pu* that prevent full occupation of the promoter during exponential growth in rich medium thus, bring about a response sooner than when they are in scarce supply. Therefore, the regulatory scenario engineered in strain *P. putida* Psal•RpoN•Pu•RBX involves both a high-capacity regime and an ultra-fast response to inducer addition.

Refactoring the XylR/*Pu* node for horizontal and vertical extension of the dose-response function

Apart of removing the auto-repression loop of XylR expression and thus producing more intracellular TF, we noticed before[39] that the PFL-engineered in genetic cassette #3 (Fig. 3) endows cells with a more digital output in response to inducer addition, i.e. ultra-sensitivity to varying effector concentrations[39]. On this basis, we wondered whether this property, which is endowed by the specific structure of the PFL of the [*Pu-xylR*] module is preserved in *P. putida* Psal•RpoN•Pu•RBX, which harbours both engineered cassettes [*Pu-xylR*] and [*Psal-rpoN*]. To answer this question, we measured the bioluminescence of *P. putida* RBX and *P. putida* Psal•RpoN•Pu•RBX with increasing concentrations of 3MBA. The data were fitted to a Hill function to gain an approximation of the dose-response relationship in either regulatory scenario (Fig. 8). A comparison of the adjusted parameters shows that the dose-response curves of both strains exhibit a different behaviour ($p < 0.0001$) in which the combined *P. putida* Psal•RpoN•Pu•RBX strain gains in inducer sensitivity and responsiveness. Nevertheless, the comparison between both Hill slope values indicated that the steepness dose/response curves did not change with the strain (p value = 0.7356). This indicated that the dynamic properties of the PFL embodied in the [*Pu-xylR*] module are preserved, but not further increased upon combination with an augmented level of σ^{54}. Taken together, the results of Fig. 8 signify that overproduction of both XylR and σ^{54} in the fashion described in this work expands the dose-response curve vertically (ultra-responsiveness) while producing at the same time a horizontal scaling[44].

Conclusion. In this work we show that artificially up-regulating σ^{54} levels of *P. putida* through an external signal and likewise increasing XylR concentration through an auto-inducible and σ^{54}-dependent positive forward loop surmounts much of the physiological limits that constrains *Pu* activity *in vivo.* This creates a non-natural but still sustained high-capacity regime that probably reflects the maximum activity that the promoter can have and thus engages its full functional space. This is plausibly caused by the complete occupation of the binding sites for both XylR and σ^{54}-RNAP *in vivo*. These are typically not saturated because of the low concentrations of these two actors and the competition for the same DNA sequences by other cellular proteins. But regardless of mechanistic details, we show here that entering two genetic amplifiers for *xylR* and *rpoN* endows the *Pu* promoter with a superior performance by all criteria: higher net transcriptional output, better inducibility and an ultra-fast response along with a

vertical extension of the dose-response curve[44, 45]. Yet, following the terminology of Ang et al[44], note that *better inducibility* does not mean necessarily *ultra-sensitivity*, but *expanded dynamic range*, i.e the regulatory node as a whole responds better to lower inducer concentrations.

As shown in Fig. 9, the functional space of the XylR/*Pu* regulatory device can be abstracted as an object bounded by the individual thresholds imposed by the two limiting regulatory elements (XylR and σ^{54}). One can then picture a growing expansion of the same space through uplifting of either constrain. However, the boundaries cannot enlarge beyond the extant limits by just defeating one of the two thresholds and leaving the other element as it was. Since the *Pu* promoter is encoded in a transmissible plasmid [11], it is possible that constraints imposed by the host (e.g. levels of σ^{54}) vary from one species to the other, an issue that deserves further studies. In any case, only concerted escalation of both components XylR and σ^{54} can lead the system to occupy its full potential space. While this is unlikely to happen in naturally evolved systems, rational rewiring of the key components (as we have done here) allows taking the performance of such systems to their limits. This is of considerable interest for designing e.g. whole cell biosensors and heterologous expression devices in which the signal-response ratio is to be exacerbated for a more efficient performance of the thereby repurposed regulatory node[46-48].

EXPERIMENTAL

Strains, culture conditions, and general procedures

The four *P. putida* strains used in study (Table 1) are derivatives of the reference strain KT2440 inserted with various combinations of the genetic cassettes indicated in each case. *E. coli* CC118λ*pir* was used as the host for propagating plasmids based on a R6K origin of replication[49]. Bacteria were grown in Luria-Bertani (LB) medium and handled with habitual Laboratory procedures[50]. When required, the media was amended with specified concentrations of 3-methylbenzylalcohol (3MBA) or saturating vapours of *m*-xylene. Antibiotics were used at the following concentrations: piperacilin (Pip) 40 µg/ml, chloramphenicol (Cm) 30 µg/ml, gentamycin (Gm) 10 µg/ml, kanamycin (Km) 50 µg/ml, and potassium tellurite (Tel) at 80 µg/ml. For PCR reactions, 50-100 ng of the DNA template indicated in each case was mixed in a 100 µl mixture with 50 pmol of each of the primers specified and 2.5 units of Pfu DNA

polymerase (Stratagene). Samples were then subject to 30 cycles of 1 min at 95°C, 1 min at 58°C and 3 min at 72°C. Clones were first checked by colony PCR[50] using 1.25 units Taq DNApolymerase (Roche) and later confirmed by DNA sequencing. Other gene cloning techniques and Molecular Biology procedures were carried out according standard methods[50].

Genetic constructs

Hybrid transposons bearing a *Pu-luxCDABE* reporter system[39, 51], a cassette expressing *xylR* under the control of its native P_R promoter[51] and a DNA segment in which *xylR* transcription is placed under *Pu* (i.e., subject to a self-amplifying loop[39]) have been described before. They are sketched as genetic modules #1, #2 and #3 in Fig. 3A, 3B and 3C, respectively. A fourth construct for conditional overexpression of the σ^{54} sigma factor was engineered using pCNB4[37] as the assembly vector. This is a mini-transposon delivery plasmid, allowing expression of the gene of interest under the control of the salicylate-responsive device formed by the transcriptional factor called NahR and its cognate promoter, *Psal.* pTn*5* [Psal•RpoN] plasmid was thereby constructed by cloning the promoterless *rpoN* gene of *P. putida* KT2440 (excised from expression plasmid pFH30[36]) downstream the *Psal* promoter of pCNB4. This originated the genetic module #4 shown in Fig. 3. Then, for delivering such a module from the donor *E. coli* CC118λ*pir* (pTn*5* [Psal•RpoN]) to the genome of different *P. putida* recipients we used a filter mating technique previously described[49]. Briefly, a mixture of donor, recipient and helper strain *E. coli* HB101 (pRK600) was laid on 0.45 μm filters in a 1:1:3 ratio and incubated for 8 h at 30°C on the surface of LB-agar plates. After incubation, cells were resuspended in 10 mM $MgSO_4$ in either case, and appropriate dilutions plated on M9/succinate amended with suitable antibiotics. This counter-selected the donor and helper strains and allowed growth of the *P. putida* clones that had acquired the insertion. Authentic transposition was verified checking the sensitivity of individual exconjugants to the marker of the delivery vector, piperacillin. The distribution of DNA modules #1 to #4 in the genomes of each of the *P. putida* strains used in this work is summarized in Fig. 3D and goes as follows. *P. putida* X•wt (formerly called *P. putida* BXPu-LUX14[51]) has its genome inserted with cassettes encoding *Pu-lux* (module #1) and *P_R-xylR* (module #2). *P. putida* Pu•RBX contains *Pu-lux* (module #1) and *Pu-xylR* (module #3). *P. putida* Psal•RpoN•X•wt is like *P. putida* X•wt but added with cassette *Psal-rpoN* (module #4). Finally *P. putida* Psal•RpoN•Pu•RBX is like *P. putida* Pu•RBX but added with *Psal-rpoN* (module #4).

Bioluminescence assays

To measure light emission by *P. putida* cells, 2 ml of each culture were first pre-grown overnight in LB at 30ºC, diluted to an OD_{600} of 0.05 and re-grown up to an OD_{600} ~ 1.0. At that point samples were exposed to either saturating vapours of *m*-xylene or increasing concentrations of 3MBA added to the growth medium as indicated in each case. For dose-response studies 200 µl aliquots of the cultures treated with 3MBA, were placed in 96 well plates (NUNC) and light emission and OD_{600} measured in a Victor II 1420 Multilabel Counter (Perkin Elmer). In the case of samples exposed to *m*-xylene, 200 µl aliquots were recovered of the culture flasks, placed the same microtiter plates and light emission and OD_{600} recorded as before. The specific bioluminescence values were the result of dividing total light emission (in arbitrary units) by the optical density of the culture (OD_{600}). Figures shown through the article represent the average of at least three biological replicates.

Protein techniques

SDS-PAGE was performed by standard protocols[50] using the Miniprotean system (Bio-Rad). Whole-cell protein extracts were prepared by harvesting the cells (10,000 × *g*, 5 min) from 1 to 20 ml of cultures (depending of the OD_{600}) in LB and resuspending the pellets in 100 µl Tris HCl 10 mM pH 7.5. Next 2× SDS-sample buffer (Tris–HCl 120 mM pH 6.8, SDS 2%, w/v, glycerol 10%, v/v, bromophenol blue 0.01%, w/v, 2-mercapto-ethanol 2%, v/v) was added to the samples, boiled for 10 min, sonicated briefly (~5 s) and centrifuged (14,000 × *g*, 10 min). Samples with thereby prepared extracts equivalent to ~10^8 cells were loaded per lane. After the electrophoresis they were transferred to a polyvinylidene difluoride membrane and blocked for 2 h at room temperature with MBT buffer (0.1% Tween and 5% skim milk in phosphate-buffered saline, PBS). For immunodetection of σ^{54}, we used the previously described recombinant antibody scFv C2[34]. Membranes were incubated with 20 ml of MBT-buffer containing 500 ng of scFv C2 for 1 hour. Unbound antibodies were eliminated by four washing steps of 5 min in 40 ml of PBS, 0.1% (v/v) Tween 20. Next, anti-E-tag-MAb-POD conjugate (1 mg/ml diluted 1:5000 in MBT-buffer, Amersham Pharmacia Biotech) was added for detecting the bound scFvs. After 1 h incubation, the membranes were washed five times with PBS/0.1% (v/v) Tween 20. The protein band corresponding to σ^{54} was developed with a chemoluminescent substrate (ECL; Amersham Pharmacia Biotech).

Modelling

Models presented in this work we made by setting a number of ordinary differential equations describing the TOL control network. Simulations and other calculations were done with MATLAB®. (See Supplementary Methods for further details). Dose-response curve analyses were performed by using GraphPad Prism version 5.00, GraphPad Software, www.graphpad.co

ACKNOWLEDGEMENTS

We thank Matthew Livesey for careful reading of the manuscript and Silvia Fernández for constructing pTn*5* [Psal•RpoN] plasmid. This work was supported by the BIO Program of the Spanish Ministry of Economy and Competitiveness, the ST-FLOW, EVOPROG and ARISYS Contracts of the EU, the ERANET-IB program and the PROMT Project of the CAM.

REFERENCES

1. D. J. Lee, S. D. Minchin and S. J. W. Busby, *Ann Rev Microbiol*, 2012, 66, 125-152.
2. M. N. Price, A. M. Deutschbauer, J. M. Skerker, K. M. Wetmore, T. Ruths, J. S. Mar, J. V. Kuehl, W. Shao and A. P. Arkin, *Mol Sys Biol,* 2013, 9, 660.
3. K. Shimizu, *ISRN Biochemistry*, 2013, 2013, 645983
4. I. Cases and V. de Lorenzo, *Nat Rev Microbiol*, 2005, 3, 105-118.
5. D. Lalaouna, M. Simoneau-Roy, D. Lafontaine and E. Masse, *Biochim Biophys Acta*, 2013, 1829, 742-747.
6. J. C. Perez and E. A. Groisman, *Cell*, 2009, 138, 233-244.
7. E. Balleza, L. N. López-Bojorquez, A. Martínez-Antonio, O. Resendis-Antonio, I. Lozada-Chávez, Y. I. Balderas-Martínez, S. Encarnación and J. Collado-Vides, *FEMS Microbiol Revs*, 2009, 33, 133-151.
8. M. E. Wall, W. S. Hlavacek and M. A. Savageau, *Nat Rev Genet*, 2004, 5, 34-42.
9. R. Silva-Rocha and V. de Lorenzo, *Ann Rev Microbiol*, 2010, 64, 257-275.
10. S. A. F. T. Van Hijum, M. H. Medema and O. P. Kuipers, *Microbiol Mol Biol Rev*, 2009, 73, 481-509.

11. J. L. Ramos and S. Marques, *Ann Rev Microbiol*, 1997, 51, 341-373.
12. P. Domínguez-Cuevas and S. Marqués, in *Handbook of Hydrocarbon and Lipid Microbiology*, ed. K. Timmis, Springer Berlin Heidelberg, 2010, 78, pp. 1127-1140
13. R. Silva-Rocha, H. de Jong, J. Tamames and V. de Lorenzo, *BMC Syst Biol*, 2011, 5, 191.
14. R. Silva-Rocha and V. de Lorenzo, *Mol BioSyst*, 2011, 7, 2982-2990.
15. E. Morett and L. Segovia, *J Bacteriol*, 1993, 175, 6067-6074.
16. V. Shingler, *Mol Microbiol*, 1996, 19, 409-416.
17. V. Shingler, *FEMS Microbiol Revs*, 2011, 35, 425-440.
18. R. Calb, A. Davidovitch, S. Koby, H. Giladi, D. Goldenberg, H. Margalit, A. Holtel, K. Timmis, J. M. Sanchez-Romero, V. de Lorenzo and A. B. Oppenheim, *J Bacteriol*, 1996, 178, 6319-6326.
19. M. Valls, R. Silva-Rocha, I. Cases, A. Munoz and V. de Lorenzo, *Mol Microbiol*, 2011, 82, 591-601.
20. J. Perez-Martin and V. de Lorenzo, *J Mol Biol*, 1996, 258, 575-587.
21. E. Rescalli, S. Saini, C. Bartocci, L. Rychlewski, V. De Lorenzo and G. Bertoni, *J Biol Chem* 2004, 279, 7777-7784.
22. E. Vitale, A. Milani, F. Renzi, E. Galli, E. Rescalli, V. de Lorenzo and G. Bertoni, *Molecular microbiology*, 2008, 69, 698-713.
23. S. Marqués, M. T. Gallegos, M. Manzanera, A. Holtel, K. N. Timmis and J. L. Ramos, *Mol Microbiol*, 1998, 180, 2889-2894.
24. G. Bertoni, S. Marques and V. de Lorenzo, *Mol Microbiol*, 1998, 27, 651-659.
25. G. Bertoni, J. Perez-Martin and V. de Lorenzo, *Mol Microbiol*, 1997, 23, 1221-1227.
26. G. Bertoni, N. Fujita, A. Ishihama and V. de Lorenzo, *EMBO J*, 1998, 17, 5120-5128.
27. M. Carmona, V. de Lorenzo and G. Bertoni, *J Biol Chem*, 1999, 274, 33790-33794.
28. R. Macchi, L. Montesissa, K. Murakami, A. Ishihama, V. De Lorenzo and G. Bertoni, *J Biol Chem*, 2003, 278, 27695-27702.
29. M. Carmona, S. Fernandez, M. J. Rodriguez and V. de Lorenzo, *J Bacteriol*, 2005, 187, 125-134.
30. L. M. Bernardo, L. U. Johansson, E. Skarfstad and V. Shingler, *J Biol Chem* 2009, 284, 828-838.
31. S. Osterberg, T. del Peso-Santos and V. Shingler, *Ann Rev Microbiol*, 2011, 65, 37-55.
32. L. M. Bernardo, L. U. Johansson, D. Solera, E. Skärfstad and V. Shingler, *Mol Microbiol*, 2006, 60, 749-764.
33. R. Silva-Rocha and V. de Lorenzo, *Environ Microbiol*, 2013, 15, 271-286.
34. P. Jurado, L. A. Fernández and V. de Lorenzo, *J Bacteriol*, 2003, 185, 3379-3383.

35. S. Fraile, F. Roncal, L. A. Fernandez and V. de Lorenzo, *J Bacteriol*, 2001, 183, 5571-5579.
36. I. Cases, V. de Lorenzo and J. Perez-Martin, *Mol Microbiol*, 1996, 19, 7-17.
37. V. de Lorenzo, S. Fernandez, M. Herrero, U. Jakubzik and K. N. Timmis, *Gene*, 1993, 130, 41-46.
38. A. Cebolla, C. Sousa and V. de Lorenzo, *Nucl Acids Res*, 2001, 29, 759-766.
39. A. de Las Heras, S. Fraile and V. de Lorenzo, 2012, *PLoS Genetics,* 8, e1002963.
40. S. Berthoumieux, H. de Jong, G. Baptist, C. Pinel, C. Ranquet, D. Ropers and J. Geiselmann, *Mol Syst Biol*, 2013, 9, 11.
41. G. W. Li, D. Burkhardt, C. Gross and J. S. Weissman, *Cell*, 2014, 157, 624-635.
42. R. Silva-Rocha and V. de Lorenzo, *Mol Microbiol*, 2012, 86, 199-211.
43. M. Valls and V. de Lorenzo, *Nucl Acids Res*, 2003, 31, 6926-6934.
44. J. Ang, E. Harris, B. J. Hussey, R. Kil and D. R. McMillen, *ACS Synth Biol*, 2013, 2, 547-567.
45. R. Hermsen, D. W. Erickson and T. Hwa, *PLoS Comput Biol*, 2011, 7, e1002265.
46. M. R. Atkinson, M. A. Savageau, J. T. Myers and A. J. Ninfa, *Cell*, 2003, 113, 597-607.
47. S. Basu, Y. Gerchman, C. H. Collins, F. H. Arnold and R. Weiss, *Nature*, 2005, 434, 5.
48. J. Garmendia, A. de las Heras, T. C. Galvao and V. de Lorenzo, *Microb Biotech*, 2008, 1, 236-246.
49. V. de Lorenzo and K. N. Timmis, *Methods Enzymol*, 1994, 235, 386-405.
50. J. Sambrook, E. F. Fritsch and T. Maniatis, *Molecular Cloning: A laboratory manual*, Cold Spring Harbor, New York, 1989.
51. A. de Las Heras, C. A. Carreño and V. de Lorenzo, *Environ Microbiol* 2008, 10, 3305-3316.

Table 1. Strains and plasmids

Strains	Relevant characteristics	Reference
E. coli CC118 λ *pir*	*E. coli* CC118 lysogenized with λ *pir* phage for hosting plasmids with an *oriV* R6K	49
E. coli DH5α	Routine cloning host strain	50
P. putida X•wt	Formerly called *P. putida* BXPu-LUX14. *P. putida* strain bearing a chromosomal *Pu-luxCDABE* fusion and *xylR* under the control of its own P_R promoter (innate negative feedback loop)	51
P. putida Pu•RBX	*P. putida* strain bearing a chromosomal *Pu-luxCDABE* fusion and *xylR* under the control of *Pu* (positive feedback loop)	39
P. putida Psal•RpoN•X•wt	*P. putida* X•wt expressing a surplus of *rpoN* under the control of a salicylate-inducible NahR/*Psal* regulatory system	This study
P. putida Psal•RpoN•Pu•RBX	*P. putida* Pu•RBX expressing a surplus of *rpoN* under the control of a salicylate-inducible NahR/*Psal* regulatory system	This study
Plasmids		
RK600	*oriV* ColE1, RK2 *mob*$^+$ *tra*$^+$, helper plasmids for tripartite matings	49
pCNB4	Mini-Tn*5* delivery vector carrying the NahR/*Psal* regulatory system	37
pFH30	Broad host range expression plasmid for the *rpoN* gene of *P. putida* engineered with an improved ribosome binding site	36
pTn*5* [Psal•RpoN]	Mini-Tn*5* delivery vector carrying the NahR/*Psal* regulatory system controlling *rpoN* expression	This study

FIGURES

Figure 1. Principal components of the XylR/*Pu* regulatory node.

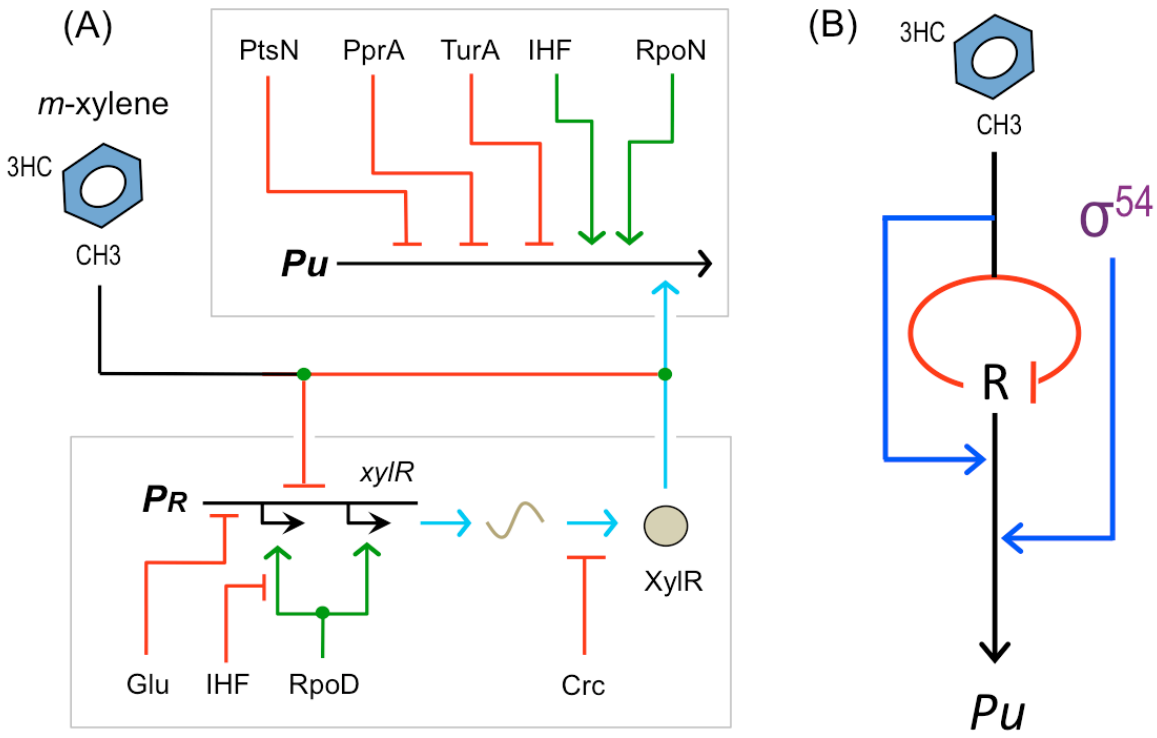

(A) Model organization of the *Pu* protomoter. The upper box represents all the main regulatory interactions (PtsN, PprA, TurA, IHF and RpoN) that play a role in the functioning of the *Pu* Promoter. The lower box represents the signals that are integrated through the P_R promoter for XylR expression. This TF is the specific regulator of the TOL system and, in the presence of *m*-xylene, triggers activation of *Pu* while, at the same time, inhibits its own expression *via* its inhibitory action on the P_R promoter. Signals are integrated at either the transcriptional or the translational level and can be positive (activation) or negative (repression) as indicated. (B) Relational scheme of the key components of the XylR/*Pu* regulatory node. The presence *m*-xylene generates an active form of XylR (R) that simultaneously turns on transcription from *Pu* but also inhibits expression of the *xylR* gene. In this natural configuration, σ^{54} is a necessary factor for expression of *Pu* but its input comes separately from the rest of the components. Positive actions in the regulatory node are maked in blue, negative counterparts in red.

Figure 2. Modeling the XylR/*Pu* regulatory node with alternative configurations of σ^{54} expression.

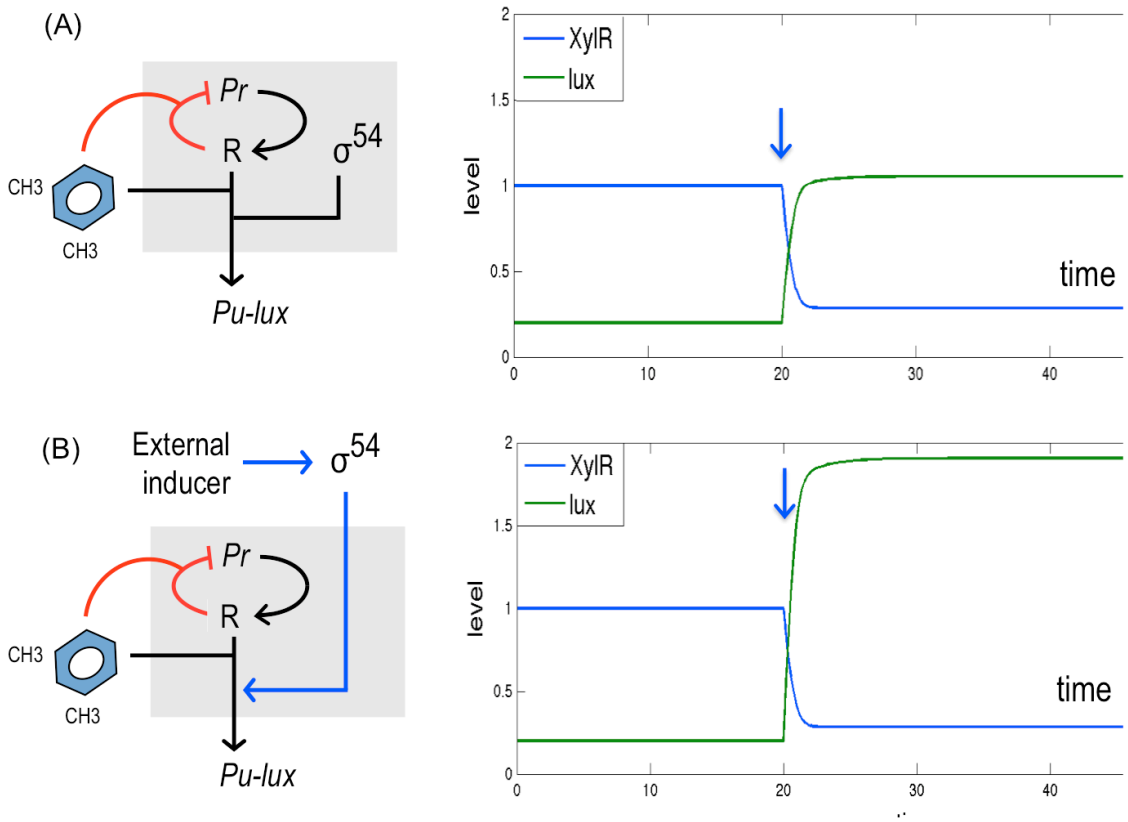

(A) Relational map of the components of the node in the native regulatory scenario. In the presence of *m*-xylene XylR and the σ^{54}-RNA polymerase trigger a *Pu-lux* reporter system, while *xylR* expression is simultaneously lowered because of the action of XyR on promoter P_R. A dynamic simulation of this case is shown to the right, arrows signaling the moment of induction by *m*-xylene. (B). Relational map in a regulatory scenario where σ^{54} is augmented through a separate external inducer. The corresponding simulation is shown as before

Figure 3. Genetic constructs and strains.

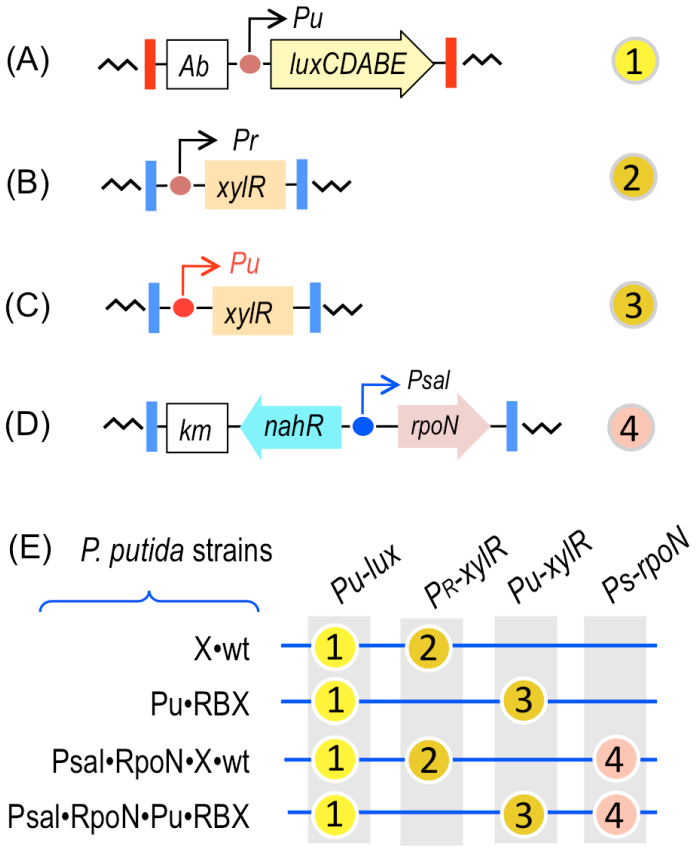

The figure shows a sketch (not a scale) of the four genetic modules born by the *P. putida* strains used in this study. (A) The *Pu-luxCDABE* reporter cassette #1 has a promoterless luminescence-determining operon controlled by the *Pu* promoter. (B) Cassete #2 has *xylR* expressed through its native promoter P_R as it appears in the TOL plasmid pWW0. (C) Cassette #3 determines *xylR* transcription engineered in an auto-activation loop that is caused by having the gene transcribed through the *Pu* promoter (D) Cassette #4 is an specialized module in which expression of the the *rpoN* gene (encoding σ^{54}) has been placed under the control of the salicylate-inducible NahR/*Psal* system. (E) *P. putida* strains used in this study with a description of the modules that they carry integrated in the chromosome by means of specialized transposons.

Figure 4. Effect of increasing σ^{54} in strains *P. putida* X•wt and *P. putida* Psal•RpoN•X•wt.

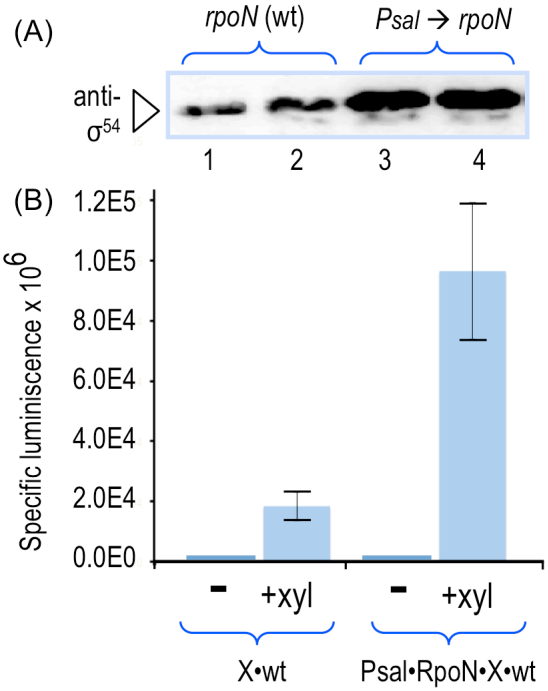

(A) Western blot of *P. putida* X•wt (wild-type levels of *rpoN*) and Psal•RpoN•BX (*Psal-rpoN*) extracts prepared from cells collected 6 hours after exposing culures to saturating vapors of *m*-xylene and probed with an anti- σ^{54} antibody. (B) Specific bioluminescence produced by the *P. putida* strains X•wt and Psal•RpoN•X•wt in the same conditions.

Figure 5. *Pu* output dynamics in *P. putida* X•wt and *P. putida* PsaI•RpoN•X•wt.

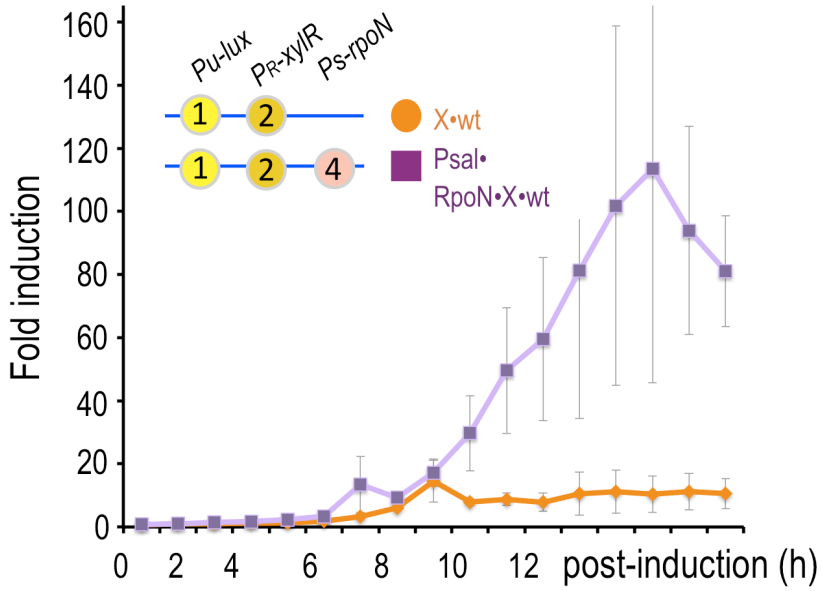

The insert specifies the genetic modules present in each strain. Bacteria were grown in the presence of salicylic and added with the XylR effector 3MBA as explained in the Experimental section.

Figure 6. Modeling the reshaped XylR/*Pu* regulatory node with an alternative configuration of σ^{54} expression.

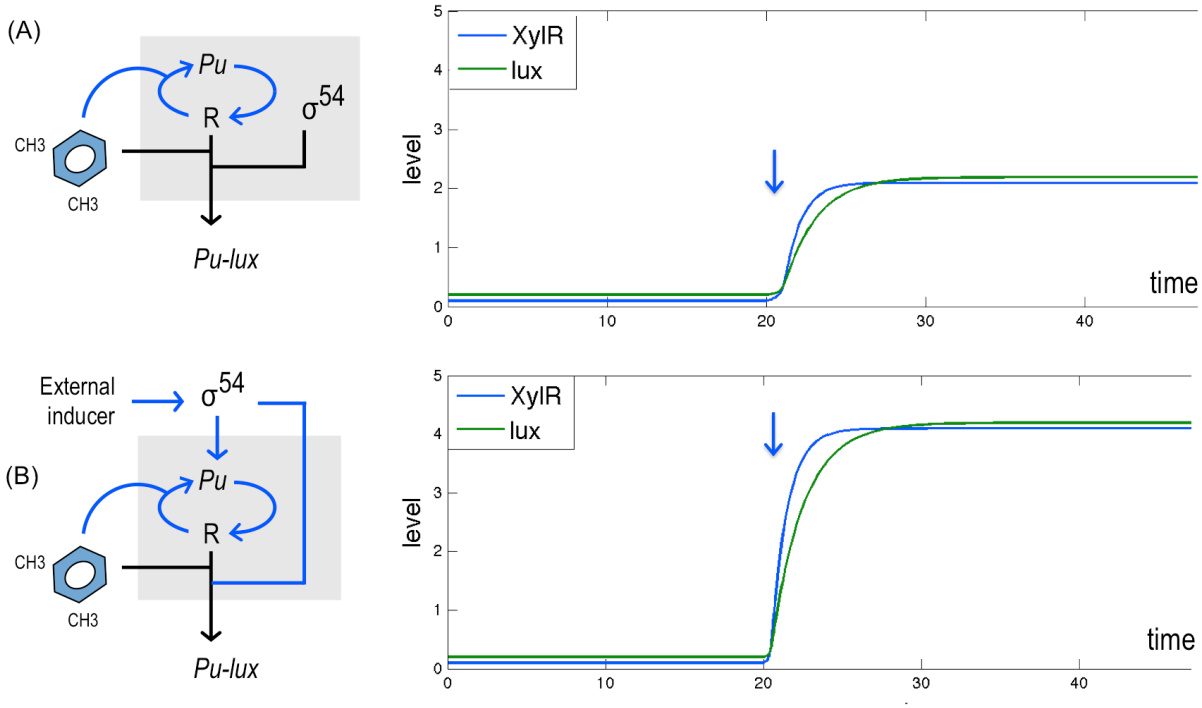

(A) Map of the node in a regulatory scenario where, in the presence of *m*-xylene, *xylR* (R) both turns *Pu* on and self-activates its expression through the *Pu* promoter also. The simulated dynamic profiles of *xylR* expression and *Pu* output with a non-variant amount of σ^{54} are shown. (B) Same, but having σ^{54} (and thus the share of σ^{54}-RNAP) augmented through an external inducer. Note that this last case enters positive signals at both sites of the node.

Figure 7. XylR/*Pu* output dynamics in *P. putida* strains Pu•RBX and Psal•RpoN•Pu•RBX.

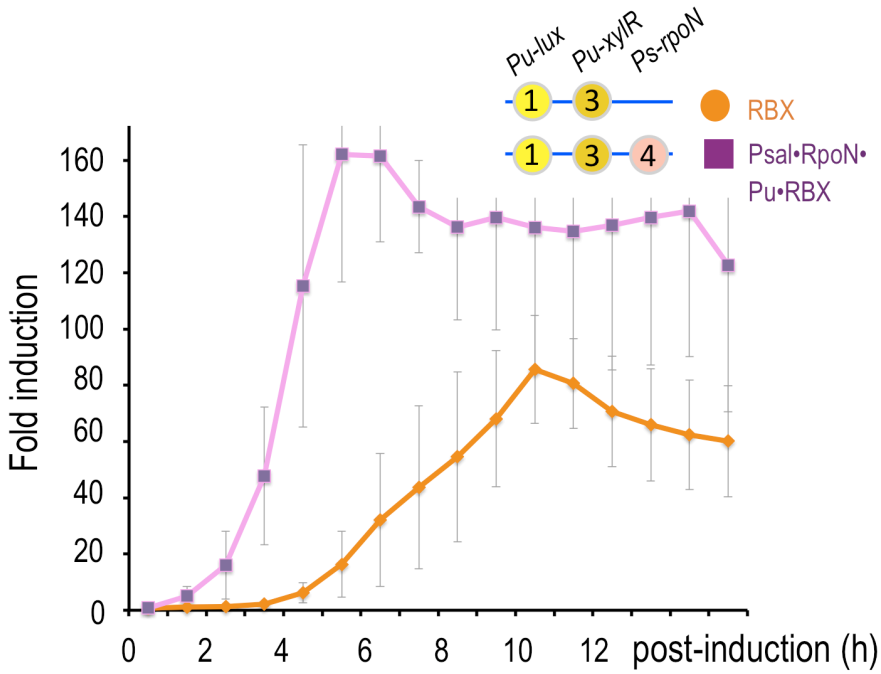

Bacteria were grown in the presence of salicylic acid and added 3MBA (see Experimental). The genetic modules present in each strain are indicated.

Figure 8. Dose-response curve of the XylR/*Pu* regulatory node under a high-capacity regime.

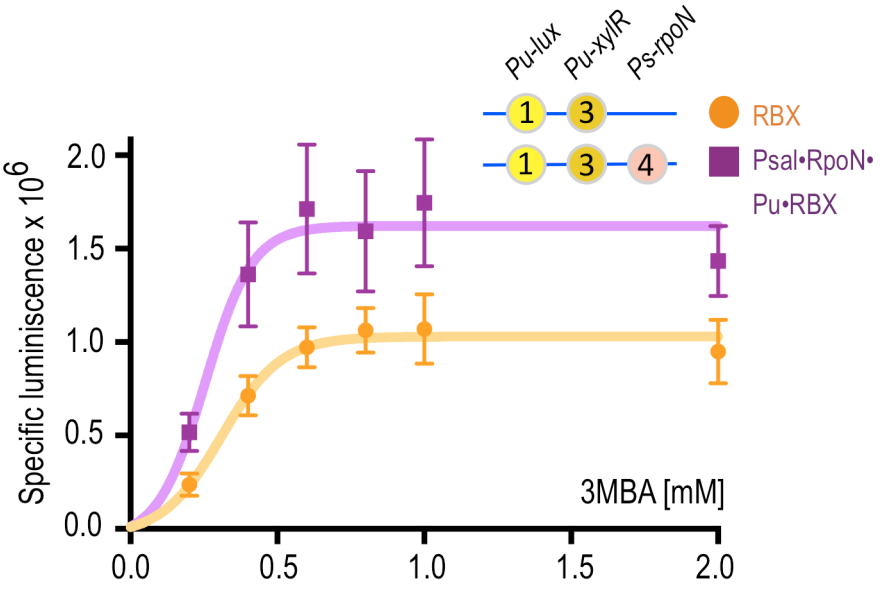

The plot shows the bioluminiscence emitted by *P. putida* Pu•RBX and *P. putida* Psal•RpoN•Pu•RBX grown in the presence of salicylic acid and added with different concentrations of 3MBA. The genetic modules present in each strain are indicated.

Figure 9. Schematic representation of the functional space of the XylR/*Pu* device under different regulatory regimes.

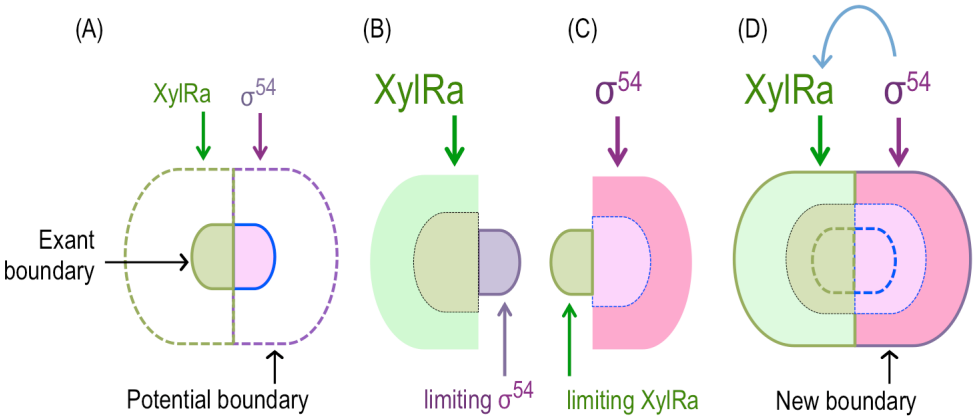

(A) The outer boundary of the system could be represented as the result of two different and mutually limiting contributors: activated XylR (XylRa, green) and σ^{54}-RNAP (σ^{54}, purple). The potential boundary of the functional space is not filled because XylRa and σ^{54}-RNAP inputs are bounded by individual thresholds of either component. These boundaries may improve, but not reach their upper limits by just overcoming constraints of one of the two actors, either XylRa (B) or σ^{54} (C). Only concerted escalation of both components can lead the system to occupy its full potential space (D).